

# Mean-field hard-core model of interference in ad-hoc wireless networks

Toshiyuki Tanaka<sup>1</sup> and K. Shashi Prabh<sup>2</sup>

**Abstract**—In this paper we present a mean-field hard-core model of interference in wireless networks using CSMA. We consider  $d$ -regular random graph ensembles in which the edges are drawn randomly and an edge in a graph represents hard-core interaction such that the two nodes connected by the edge cannot be simultaneously active, or transmitting. We present an analysis of average activity in the presence of hard-core interactions in conflict graphs sampled from regular random graph ensembles. We also present experimental data obtained using Monte-Carlo simulations. A surprising conclusion of experimental results is that the average activity is not always monotonic in  $d$ .

## I. INTRODUCTION

Modeling and analysis of ad-hoc networks have drawn significant attention of researchers from networking as well as information theory. Interference is the quintessential issue in modeling and analysis of wireless networks. Interference limits capacity and leads to performance penalties, such as throughput loss, increased delay and energy wastage. Medium access control (MAC) protocols limit, or even eliminate, collisions by determining the subset of nodes that can be transmitting simultaneously. The MAC protocols used in ad-hoc networks are distributed. Carrier Sense Multiple Access (CSMA) is such a MAC protocol that is very commonly used. Prior to initiating a transmission, a node performs carrier sensing in CSMA. A transmission is started only if the medium is free. In practice, medium is deemed to be free if carrier sensing returns a value below some specified threshold. If the medium is found to be busy, the transmitting node backs-off and performs carrier sensing again but after elapse of certain time. Although CSMA is somewhat old [1], there has been renewed interest in the analysis of CSMA, primarily because of recent research results as well as development of new wireless systems using CSMA, such as cognitive radio.

<sup>1</sup>Toshiyuki Tanaka is with Graduate School of Informatics, Kyoto University, Yoshida Hon-machi, Sakyo-ku, Kyoto, 606-8501 Japan. [tt@i.kyoto-u.ac.jp](mailto:tt@i.kyoto-u.ac.jp)

<sup>2</sup>Shashi Prabh is with School of Engineering, Shiv Nadar University, Dadri, Gautam Budh Nagar, UP 201314, India. [shashi.prabh@snu.edu.in](mailto:shashi.prabh@snu.edu.in)

Statistical modeling of blocking caused by interference can be done in several different ways. One approach consists of using stochastic geometry [2] where locations of wireless nodes are represented in terms of a spatial point process [3], [4]. Matérn hard-core point processes (HCPP) [5] are point-process models that have extensively been studied. They are defined on the basis of Poisson point processes (PPPs). Matérn type I process is defined by first generating a set of points in  $\mathbb{R}^n$  using a PPP with a spatially-uniform intensity, and then by eliminating all the points that have other points with distance less than the hard-core distance  $\delta$ . Matérn type II process can be regarded as a dynamical variant of Matérn type I process. It is defined by generating points in  $\mathbb{R}^n$  according to a PPP sequentially, and eliminating all the points that have other points generated earlier with distance less than the hard-core distance  $\delta$ . A key assumption behind the modeling of interference with HCPP is that occurrence of interference is determined geometrically: two nodes interfere if the distance between them is less than  $\delta$ , and they do not if the distance is more than  $\delta$ . Some results on analysis of interference using HCPP can be found in [6], [7], [8], [9], [10].

Another approach, which we pursue here, is the mean-field modeling. The conventional notion of the mean-field method, as described in statistical-physics textbooks such as [11], is that the thermodynamics of the state of an entity, e.g., energy of an individual atom, is determined using long-range order parameter, e.g., the average energy of the system while ignoring local fluctuations. Instead, we use this term in the context of the framework of statistical mechanics of disordered systems (“spin glasses”) applied to informatics problems [12], [13], where mean-field models are characterized as models which lack any geometrical structure that would otherwise be present in models defined on finite-dimensional spaces, and which, thanks to the lack of geometrical structure, admit exact expressions for macroscopic quantities in the large-system limit.

In our mean-field approach to analyzing ad-hoc networks, one therefore completely ignores geometrical aspects. One can argue that ignoring geometrical as-

pects is justifiable to a certain extent under scattering-rich environments, where the distance is not an appropriate measure for interference strength. Further, our simulation shows that the results obtained by the mean-field approach are very good approximation of the case when one takes the spatial geometry into account. In our mean-field modeling, we consider a random graph ensemble in which a graph instance consists of many nodes and randomly drawn edges among them. An edge in a graph represents hard-core interaction such that the two nodes connected by the edge cannot be simultaneously active (transmitting). In the mean-field hard-core model that we discuss in this manuscript, we specify a degree distribution and consider the large-system limit, where the number of nodes is sent to infinity, in order to allow statistical-mechanics analysis of such models. A comprehensive review of the studies on such models can be found in [14].

## II. MODEL

Let us consider a wireless network where CSMA is used for medium access arbitration. We model the network using a conflict graph  $G = (V, E)$  where  $V$  represents the set of nodes. The set of edges  $E$  represents the pairs of nodes that interfere. More precisely, an edge  $(i, j) \in E$  means that nodes  $i$  and  $j$  cannot be simultaneously active due to interference between them. Let  $\mathbf{s} := \{s_i \in \{0, 1\} : i \in V\}$  denote a set of configurations, with  $s_i = 1$  and  $0$  representing the state of node  $i$  being active (transmitting) and inactive, respectively.

Let

$$p(\mathbf{s}; \boldsymbol{\mu}, G) = \frac{1}{Z} \prod_{i \in V} e^{\mu_i s_i} \prod_{(i, j) \in E} (1 - s_i s_j), \quad (1)$$

where  $\boldsymbol{\mu} := \{\mu_i \in \mathbb{R} : i \in V\}$  and  $Z$  is the partition function. The probability that node  $i$  is active if the hard-core interactions  $E$  were absent is defined via the parameter  $\mu_i$  as  $\rho_{i0} := e^{\mu_i} / (1 + e^{\mu_i})$ . We thus call  $\mu_i$  the *intensity* of node  $i$ . The factor  $(1 - s_i s_j)$  represents blocking between nodes  $i$  and  $j$  so that  $s_i$  and  $s_j$  cannot simultaneously be equal to 1.

The intensity  $\mu_i$  has the following interpretation. Assume that there were no hard-core interactions, and that the state  $s_i$  of node  $i$  follows a continuous-time Markov chain with transition rates  $r_{i;0 \rightarrow 1}$  and  $r_{i;1 \rightarrow 0}$ . At equilibrium, detailed balance holds:

$$\begin{aligned} p(s_i^{(t)} = 0)p(s_i^{(t+\Delta t)} = 1 | s_i^{(t)} = 0) \\ = p(s_i^{(t)} = 1)p(s_i^{(t+\Delta t)} = 0 | s_i^{(t)} = 1), \end{aligned} \quad (2)$$

yielding

$$\begin{aligned} \frac{\rho_{i0}}{1 - \rho_{i0}} &= \frac{p(s_i^{(t)} = 1)}{p(s_i^{(t)} = 0)} = \frac{p(s_i^{(t+\Delta t)} = 1 | s_i^{(t)} = 0)}{p(s_i^{(t+\Delta t)} = 0 | s_i^{(t)} = 1)} \\ &= \frac{r_{i;0 \rightarrow 1}}{r_{i;1 \rightarrow 0}}. \end{aligned} \quad (3)$$

By the definition of the intensity  $\mu_i$ , one can let

$$e^{\mu_i} = \frac{r_{i;0 \rightarrow 1}}{r_{i;1 \rightarrow 0}}, \quad (4)$$

or equivalently,  $\mu_i = \log(r_{i;0 \rightarrow 1} / r_{i;1 \rightarrow 0})$ . If one assumes a saturated scenario, in which every node always has data to transmit, the above modeling amounts to assuming that the transmitting time and the back-off time are independent and exponentially distributed with means  $1/r_{i;1 \rightarrow 0}$  and  $1/r_{i;0 \rightarrow 1}$ , respectively. It should be noted that, even if the distributions of the transmitting time and the back-off time are not exponentially distributed, the stationary distribution of the configuration is given by (1), which was proved in [15].

Given a conflict graph  $G = (V, E)$ , the degree of node  $i \in V$  is defined as the number of edges incident to  $i$ . Let  $n_d$  be the number of nodes in  $V$  with node degree  $d \in \{0, 1, \dots\}$ . One has  $\sum_d n_d = |V|$  and  $\sum_d d n_d = 2|E|$ . The degree distribution of  $G$  is defined as  $\lambda(d) := n_d / |V|$ .

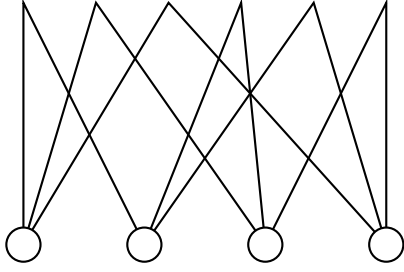
We define random graph ensemble  $\mathcal{G}(|V|, \lambda)$ , specified by the number of nodes  $|V|$  and the degree distribution  $\lambda$ , as follows. For  $d \in \{0, 1, \dots\}$  prepare  $n_d \approx |V| \lambda(d)$  nodes with degree  $d$ , and also  $|E| = (|V|/2) \sum_d d \lambda(d)$  edges. Since a node with degree  $d$  is connected to  $d$  distinct edges, and an edge connects two nodes, each graph is realized by connecting  $d$  of the  $2|E|$  end-points of distinct edges to each node (see Fig. 1). A selection of permutations of the  $2|E|$  end-points chosen uniformly randomly from all possible  $(2|E|)!$  permutations defines the random ensemble  $\mathcal{G}(|V|, \lambda)$ .

Special types of random graph ensembles are regular ensembles, where the node degrees are constant. We call a regular ensemble for which the node degrees are all equal to  $d$  a  $d$ -regular graph ensemble. In the rest of this paper, we consider  $d$ -regular ensembles.

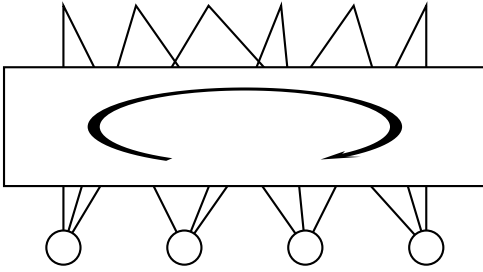
## III. INTERFERENCE ANALYSIS

For a fixed degree distribution, an instance of a random conflict graph ensemble is asymptotically free of cycles of finite length in the limit  $|V| \rightarrow \infty$ . It suggests use of belief propagation for approximately evaluating marginal probabilities

$$p(s_i; \boldsymbol{\mu}, G) = \sum_{\mathbf{s} \setminus s_i} p(\mathbf{s}; \boldsymbol{\mu}, G), \quad (5)$$



(a) A graph instance.



(b) Random permutation.

Fig. 1: Random graph ensemble.

where  $p(\mathbf{s}; \boldsymbol{\mu}, G)$  is the joint probability distribution of the configuration  $\mathbf{s}$  of node activities defined in (1). Since the configuration  $\mathbf{s}$  is a vector of binary elements, messages in belief propagation can be parametrized by their respective expectation parameters. Letting  $\{\pi_{j \rightarrow i} \in [0, 1] : (i, j) \in E\}$  denote the parameters of the messages, belief propagation equation is written as

$$\pi_{j \rightarrow i} = \frac{e^{\mu_j} \prod_{k \in N(j) \setminus i} (1 - \pi_{k \rightarrow j})}{1 + e^{\mu_j} \prod_{k \in N(j) \setminus i} (1 - \pi_{k \rightarrow j})}, \quad (6)$$

where  $N(j) \setminus i$  denotes the set of neighbors of node  $j$  in the graph  $G$  excluding node  $i$ . The belief propagation equation (6) is applied iteratively to update the messages  $\{\pi_{j \rightarrow i}\}$ , and after convergence, one obtains an estimate of the marginal probability  $p(s_i; \boldsymbol{\mu}, G)$  as

$$p(s_i; \boldsymbol{\mu}, G) \approx \frac{e^{\mu_i s_i} \prod_{j \in N(i)} (1 - \pi_{j \rightarrow i} s_i)}{1 + e^{\mu_i} \prod_{j \in N(i)} (1 - \pi_{j \rightarrow i})}. \quad (7)$$

In the following analysis we assume that  $d$  is a positive integer and that  $\mu_i = \mu$  holds for all  $i \in V$ . In this case, the above belief propagation equation is satisfied by letting  $\pi_{i \rightarrow j} = \bar{\pi}$  for all  $(i, j) \in E$ , where  $\bar{\pi}$  is the unique solution of

$$\bar{\pi} = f(\bar{\pi}; d, \mu), \quad (8)$$

where

$$f(z; d, \mu) := \frac{e^{\mu}(1-z)^{d-1}}{1 + e^{\mu}(1-z)^{d-1}} \quad (9)$$

is the message-updating formula when the incoming messages are all equal to  $z$ . The condition (8) can be further simplified to

$$\bar{\pi} = e^{\mu}(1 - \bar{\pi})^d. \quad (10)$$

Under the uniform solution  $\forall (i, j) \in E$ ,  $\pi_{i \rightarrow j} = \bar{\pi}$ , the estimated probability (7) of a node  $i$  to be communicating is independent of  $i$ , and we use  $\rho$  to denote it. One therefore has

$$\rho = \frac{e^{\mu}(1 - \bar{\pi})^d}{1 + e^{\mu}(1 - \bar{\pi})^d} = \frac{\bar{\pi}}{1 + \bar{\pi}}. \quad (11)$$

The uniform solution  $\forall (i, j) \in E$ ,  $\pi_{i \rightarrow j} = \bar{\pi}$  can be unstable under the dynamics of message updates in belief propagation. Indeed, the stability corresponds to that of a one-dimensional dynamical system

$$z^{t+1} = f(z^t; d, \mu) \quad (12)$$

around the fixed point  $z = \bar{\pi}$ . The stability condition reads

$$(d-1)\bar{\pi} < 1. \quad (13)$$

Translating the stability condition into the condition for  $\mu$ , one observes that the uniform solution  $\pi_{i \rightarrow j} = \bar{\pi}$  is stable if and only if  $\mu \leq \mu_c$ , where

$$\mu_c = (d-1) \log(d-1) - d \log(d-2). \quad (14)$$

This stability condition was first obtained in [16].

When  $\mu > \mu_c$ , the dynamical system (12) has a period-2 stable solution. It corresponds to the situation where two message values  $\bar{\pi}_+$  and  $\bar{\pi}_-$  appear alternately as the messages are propagated across the graph, where  $\bar{\pi}_{\pm} = f(\bar{\pi}_{\mp}; d, \mu)$  and  $\bar{\pi}_+ > \bar{\pi}_-$ . This argument implies that when  $\mu > \mu_c$ , belief propagation may exhibit spontaneous symmetry breaking. However, such non-uniform solutions with globally broken symmetry will be invalidated by the mere existence of cycles of odd length in the graph, and should be just an artifact. Therefore, we consider the uniform solution in the following.

It is known that, as  $\mu$  becomes even larger, the uniform solution will lose its validity. A necessary condition for the uniform solution to be valid is what is called the local stability [14], [17]. It can be derived on the basis of the radius of the disk containing the bulk of eigenvalues of a nonbacktracking matrix associated with the graph  $G$  [18], and for the  $d$ -regular ensemble it is given by

$$(d-1)\bar{\pi}^2 < 1. \quad (15)$$

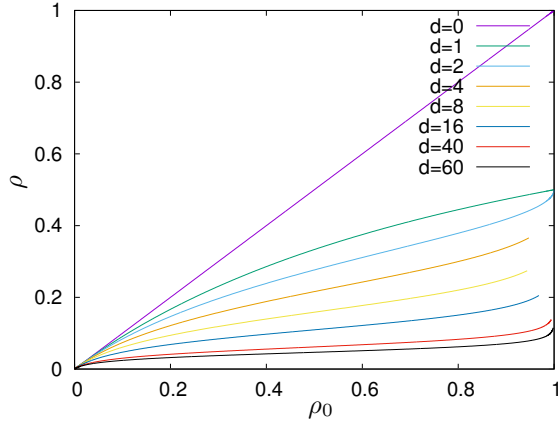


Fig. 2: The probability  $\rho$  of mean-field hard-core model versus the probability  $\rho_0$  without hard-core interactions, parametrized by degree  $d$ .

If the above local stability condition is not satisfied, more elaborate evaluations will be required.

Figure 2 shows the probability  $\rho$  of the mean-field hard-core model with degree  $d$  versus the probability  $\rho_0$  without hard-core interactions, plotted over the ranges where the local stability condition is satisfied. From this figure, one can observe that one has to resort to the elaborate analysis only when  $\rho_0$  is very close to 1. For the remaining case, which would be relevant to the application of the mean-field hard-core models to wireless network analysis, the uniform solution provides a valid description in the large-system limit.

The ratio

$$r := \frac{\rho}{\rho_0} \quad (16)$$

describes how the existence of hard-core interference would decrease the probability of nodes to be communicating. Figure 3 shows the ratio  $r$  versus  $\rho_0$  for  $d$ -regular ensembles. The slope at  $\rho_0 = 0$  is equal to  $-d$ . For  $d = 1$  the ratio  $r$  monotonically decreases from 1 to 0.5. For  $d \geq 2$ , on the other hand, the ratio  $r$  becomes minimum at  $\rho_0 \in (0, 1)$ . The minimum is characterized by the condition

$$(d+1) + (d-1)\bar{\pi} = (1-\bar{\pi})^{1-d}, \quad (17)$$

which has a unique solution in  $\bar{\pi} \in (0, 1)$  for  $d \geq 2$ . The markers in Figure 3 show the minima of  $r$ .

#### IV. NUMERICAL EXPERIMENTS

We tested the prediction accuracy of our analytical results detailed in the previous section using Monte-Carlo simulation. The main steps used in the simulation are listed in Algorithm 1. The number of nodes in simulations was 10000. The parameter  $n_{\text{flip}}$  was chosen large enough so that the system equilibrates,

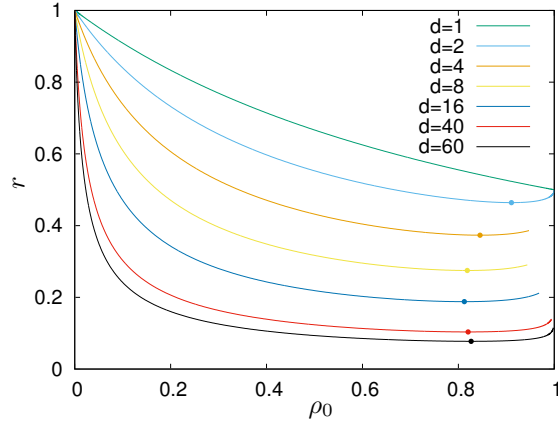


Fig. 3: Ratio  $r$  evaluated for mean-field hard-core model with degree  $d$  versus the probability without hard-core interactions,  $\rho_0$ .

and depending on the strength of fluctuation across trials, the number of trials  $N_{\text{trial}}$  varied between 150 and 300. Figure 4 shows the result where we compare the analytically obtained value of  $r$  with the simulation data. The analytical result is in close agreement with the simulation data for  $\rho_0$  upto around 0.5. Our data shows that the agreement for larger  $\rho_0$  values gets better with the increase in the degree  $d$  of regular graph ensembles. The  $d = 1$  case is an exception because this corresponds to cycle-free isolated two-node pairs where the theory becomes exact.

```

for  $N_{\text{trial}}$  times do
  Generate conflict graph;
  Mark all nodes inactive;
  for  $n_{\text{flip}}$  times do
    Select node i randomly;
    if i is inactive and flipping its state does
      not cause conflict then
      | Flip the state of i with probability rho_0
      end
    else if i is active then
      | Flip the state of i with probability
      |  $1 - \rho_0$ 
      end
    end
  end
end

```

Algorithm 1: Sketch of simulation algorithm

We also simulated two scenarios where nodes were placed on a two-dimensional square lattice and on a two-dimensional triangular lattice, respectively. Conflict graphs were generated for each degree  $d$  by adding edges to  $d$  nearest neighbors of each node

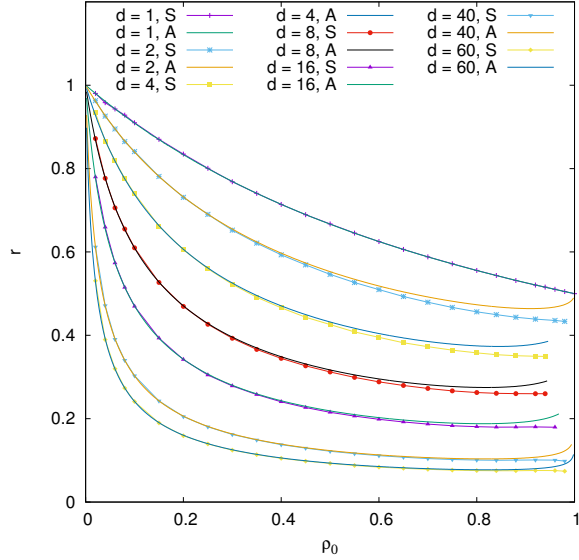
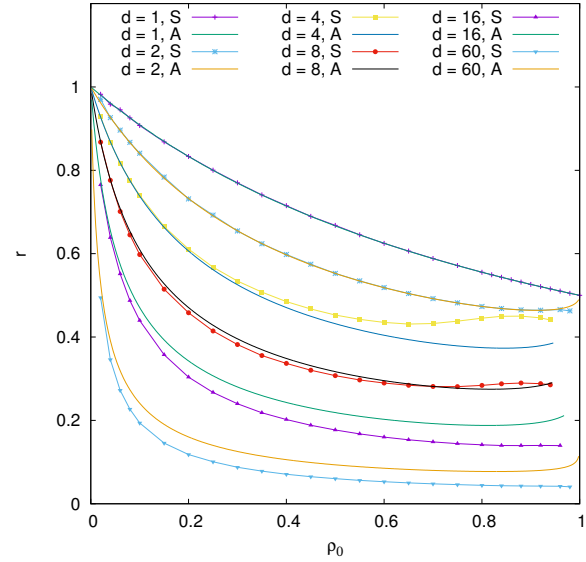


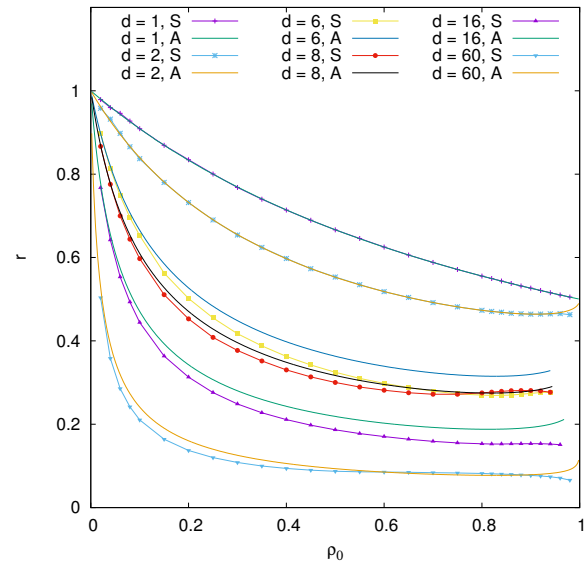
Fig. 4: Comparison of analytical result with simulation data. S and A indicate simulation and analytical data, respectively.

using  $L_1$ -norm to determine the neighbors. If  $d$  was set such that not all equidistant neighbors could be selected (e.g.,  $d = 2$ ), then a subset of neighbors was selected systematically (e.g., start from “left” neighbor, scan clockwise until specified number neighbors are found). Figure 5 shows the simulation results for these scenarios. Although the assumption underlying the analysis that the conflict graph is sampled from a regular ensemble is not valid in these scenarios, the analytical results derived earlier appear to be a good approximation for these more realistic models where interference is limited to local neighborhood.

The observed discrepancy in Fig. 5 between the analytical result and simulation is due to local geometry induced by the structure of the conflict graphs. We take a closer look at the discrepancy in the  $\rho$  versus  $\rho_0$  plots of simulation data shown in Fig. 6. One normally expects monotonic behavior of  $\rho$  versus  $\rho_0$  curves. Specifically, at a fixed  $\rho_0$ ,  $\rho(d_i)$  should not be greater than  $\rho(d_j)$  where  $d_i > d_j$ . The data shows two anomalies. The first anomaly occurs around  $\rho_0 = 0.5$  when the  $\rho$  values of a subset of different  $d$  start to converge. For the triangular lattice where nodes are packed more densely than the square lattice, this anomaly leads to a surprising behavior where, after the convergence of  $\rho$  versus  $\rho_0$  curves,  $\rho(d_i) > \rho(d_j)$  where  $d_i > d_j$ . This anomaly is quite pronounced at low  $d$  values and starts to vanish as  $d$  is increased beyond 20. The second anomaly occurs near  $\rho_0 =$



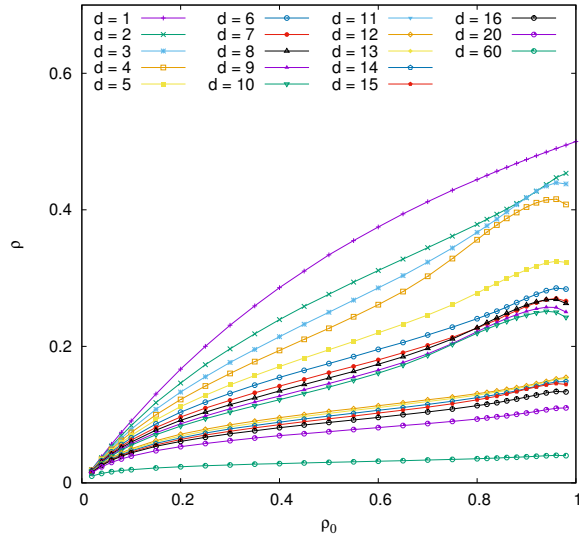
(a) Square lattice



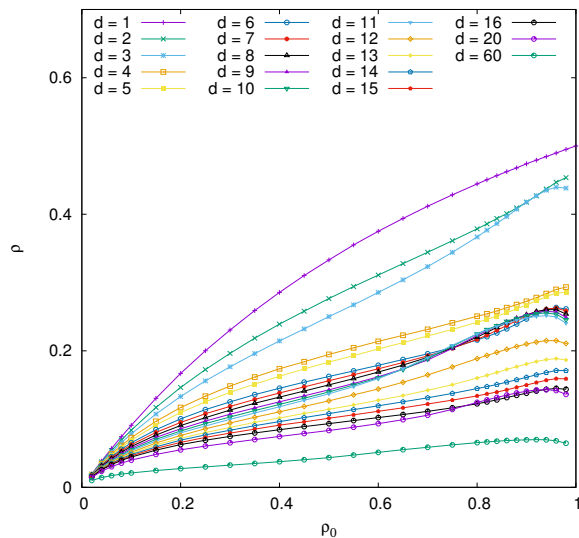
(b) Triangular lattice

Fig. 5: Comparison of the analytical result derived for random conflict graph ensemble with simulation data for localized conflict graphs. S and A indicate simulation and analytical data, respectively.

0.95 when  $\rho$  starts to decrease with increasing  $\rho_0$ . This second anomaly is present across all  $d$  values that we simulated. The first anomaly is absent in simulation data for conflict graphs generated from regular ensembles, as shown in Fig. 7.



(a) Square lattice



(b) Triangular lattice

Fig. 6: Non-monotonic behavior.

## V. CONCLUSION

We developed a mean-field hard-core model of interference in CSMA-based wireless networks. We derived expression for average activity in  $d$ -regular

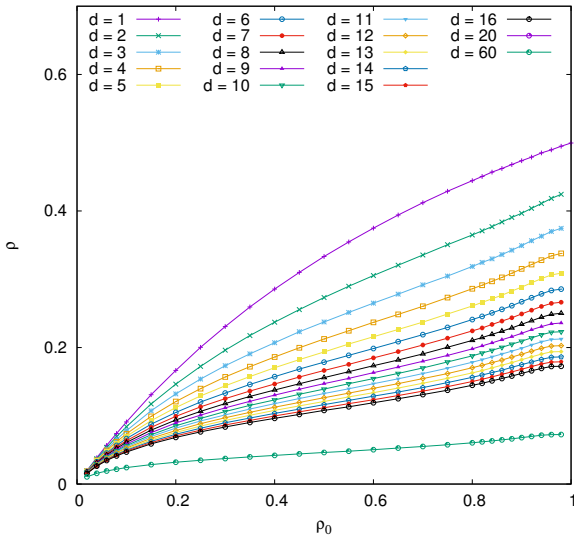


Fig. 7: Absence of the first anomaly in conflict graphs generated from regular ensembles.

ensemble of conflict graphs and evaluated its accuracy using Monte-Carlo simulations. We found that the analytical result is in very good agreement with experimental data for large  $d$ , as well as for small  $d$  and  $\rho_0 \lesssim 0.5$ . We also studied  $d$ -regular conflict graphs defined on square and triangular lattices and found existence of anomalies. Once again, the analytical result is in very good agreement with experimental data for large  $d$  but there are significant deviations for small  $d$  and  $\rho_0 \gtrsim 0.5$  owing to the anomalies. An implication of large  $d$  is dense wireless networks. Our results are primarily applicable to such networks.

## ACKNOWLEDGMENT

TT acknowledges support of the Grant-in-Aid for Scientific Research on Innovative Areas, MEXT, Japan (No. 25120008).

## REFERENCES

- [1] L. Kleinrock and F. Tobagi, "Packet switching in radio channels: Part I—carrier sense multiple-access modes and their throughput-delay characteristics," *IEEE Transactions on Communications*, vol. 23, no. 12, pp. 1400–1416, Dec. 1975.
- [2] D. Stoyan, W. Kendall, and J. Mecke, *Stochastic Geometry and its Applications*, 2nd ed. Wiley, 1995.
- [3] J. G. Andrews, R. K. Ganti, M. Haenggi, N. Jindal, and S. Weber, "A primer on spatial modeling and analysis in wireless networks," *IEEE Communications Magazine*, vol. 48, no. 11, pp. 156–163, Nov. 2010.
- [4] M. Haenggi, *Stochastic Geometry for Wireless Networks*. Cambridge University Press, 2013.
- [5] B. Matérn, *Spatial Variation*, 2nd ed., ser. Springer Lecture Notes in Statistics, 1986, vol. 36.

- [6] F. Baccelli and B. Błaszczyszyn, *Stochastic Geometry and Wireless Networks: Volume I Theory*, ser. Foundations and Trends in Networking. Now Publishers, 2009, vol. 3, no. 3–4.
- [7] —, *Stochastic Geometry and Wireless Networks: Volume II Applications*, ser. Foundations and Trends in Networking. Now Publishers, 2010, vol. 4, no. 1–2.
- [8] M. Haenggi, “Mean interference in hard-core wireless networks,” *IEEE Communications Letters*, vol. 15, no. 8, pp. 792–794, Aug. 2011.
- [9] H. ElSawy and E. Hossain, “A modified hard core point process for analysis of random CSMA wireless networks in general fading environments,” *IEEE Transactions on Communications*, vol. 61, no. 4, pp. 1520–1534, Apr. 2013.
- [10] B. Cho, K. Koufos, and R. Jäntti, “Bounding the mean interference in Matérn type II hard-core wireless networks,” *IEEE Wireless Communications Letters*, vol. 2, no. 5, pp. 563–566, Oct. 2013.
- [11] R. K. Pathria, *Statistical Mechanics*, 2nd ed. Oxford, UK: Butterworth Heineman, 1996.
- [12] H. Nishimori, *Statistical Physics of Spin Glasses and Information Processing: An Introduction*. Oxford University Press, 2001.
- [13] M. Mézard and A. Montanari, *Information, Physics, and Computation*. Oxford University Press, 2009.
- [14] J. Barbier, F. Krzakala, L. Zdeborová, and P. Zhang, “The hard-core model on random graphs revisited,” *Journal of Physics: Conference Series*, vol. 473, no. 012021, 2013.
- [15] P. M. van de Ven, S. C. Borst, J. S. H. van Leeuwen, and A. Proutière, “Insensitivity and stability of random-access networks,” *Performance Evaluation*, vol. 67, no. 11, pp. 1230–1242, Nov. 2010.
- [16] F. P. Kelly, “Stochastic models of computer communication systems,” *Journal of the Royal Statistical Society, Series B (Methodological)*, vol. 47, no. 3, pp. 379–395, 1985.
- [17] P. Zhang, Y. Zeng, and H. Zhou, “Stability analysis on the finite-temperature replica-symmetric and first-step replica-symmetry-broken cavity solutions of the random vertex cover problem,” *Physical Review E*, vol. 80, no. 2, p. 021122, 2009.
- [18] F. Krzakala, C. Moore, E. Mossel, J. Neeman, A. Sly, L. Zdeborová, and P. Zhang, “Spectral redemption in clustering sparse networks,” *Proceedings of the National Academy of Sciences of the United States of America*, vol. 110, no. 52, pp. 20 935–20 940, Dec. 2013.